Key Elements in the Structure and Function Relationship of the $MgCl_2/TiCl_4$/Lewis Base Ziegler−Natta Catalytic System

Andrea Correa,*,† Fabrizio Piemontesi,‡ Giampiero Morini,‡ and Luigi Cavallo†

Dipartimento di Chimica, Università di Salerno, Via Ponte don Melillo, Fisciano (SA), I-84084, Italy, and Centro Ricerche "Giulio Natta", Basell Poliolefine Italia, Piazzale Donegani 12, Ferrara, I-44100 Italy

Received June 11, 2007; Revised Manuscript Received August 28, 2007

ABSTRACT: We present a theoretical study of the basic interactions occurring at supported hetereogenous Ziegler−Natta catalytic systems. We first investigated the interaction between prototypes of each class of industrially relevant internal donors (1,3-diethers, alkoxysilanes, phthalates, succinates) and the $MgCl_2$ support. Our analysis indicates that donors can be separated into two classes. 1,3-Diethers and alkoxysilanes belong to the former because they have a short spacer between the coordinating O atoms and coordinate preferentially to the same Mg atom of the (110) lateral cut. Conversely, phthalates and succinates belong to the latter class because they have a longer spacer between the coordinating O atoms and thus can adopt a variety of coordination modes. Indeed, they can coordinate to both the (100) and (110) lateral cuts. In the last part of this manuscript we report on the stereo- and regioselective behavior of possible active Ti species with and without two succinate molecules coordinated in the proximity of the Ti atom. We show that the two succinate molecules confer a remarkable stereoselectivity in both primary and secondary propene insertions. This model very simply rationalizes the effect of the donors, and it is consistent with the models so far developed to rationalize the stereoselectivity of metallocene and octahedral nonmetallocene catalysts.

Introduction

The world market for polypropylene is currently over 30×10^6 tons/year, and by far the largest fraction of the global polymer is obtained with heterogeneous Ziegler−Natta catalytic systems. Over the years, these catalysts have evolved from simple $TiCl_3$ crystals into the nowadays-used $MgCl_2/TiCl_4$/donor systems, where the donor is a Lewis base that can be added during catalyst preparation (the so-called internal donor).[1] Among donors alkoxysilanes, 1,3-diethers,[2] aromatic esters (benzoates and phthalates in particular),[3,4] and recently aliphatic esters (succinates in particular) have been shown to be particularly effective.[5] Catalyst activation requires addition of alkylating reducing species ($AlEt_3$ the most used) possibly mixed with a second electron donor (the so-called external donor), usually an alkoxysilane or, more recently, a succinate. The resulting active system is of extreme chemical complexity, and the polypropylenes obtained present very different properties.

The nature of the added Lewis bases is fundamental in terms of performances, since it can strongly modify (i) the tacticity of the obtained polypropylenes from a large fraction of almost atactic polymer (as in the absence of any Lewis base) to almost exclusively highly isotactic polymers; (ii) the molecular masses distribution, that can be rather narrow or rather broad; (iii) the response to molecular hydrogen, which clearly allows one to control the molecular masses of the produced polymers.[6−17] The Lewis bases have been suggested to stabilize small primary crystallites of $MgCl_2$ and/or to influence the amount and distribution of $TiCl_4$ in the final catalyst. Indeed, the donor has to compete with $TiCl_4$ to coordinate on the $MgCl_2$ surfaces, possibly inducing formation of the more stereoselective sites. Additionally, the internal donor could poison poorly stereoselective sites or could transform aspecific sites in highly stereoselective sites.

Of course, several studies focused on the characterization of heterogeneous Ziegler−Natta catalysts,[16,18−38] but definitive answers have not been achieved yet. Nevertheless, some points are well accepted now. The primary particles of activated $MgCl_2$ are composed of a few irregularly stacked Cl−Mg−Cl sandwichlike monolayers,[39] with the $MgCl_2$ microcrystals terminated by the (100) and (110) lateral cuts.[27,40] For electroneutrality reasons, these two lateral cuts contain coordinatively unsaturated Mg^{2+} ions with coordination numbers 4 and 5 on the (110) and (100) cuts, respectively, as shown in Figure 1.[40,41]

Knowledge of the catalyst structure prior and after reduction with Al−alkyl compounds is also incomplete. Corradini and co-workers proposed that preferential titanium−chlorides coordination would occur on the lateral cuts, leading to adsorbed monomeric Ti species on the (100) and (110) cuts and to dimeric Ti species on the (100) cut.[40] These Ti(IV) and Ti(III) species could be epitaxially adsorbed on the (110) and (100)-cuts. In the case of the (100)-lateral cut, monodimensional $Ti(III)Cl_3$ clusters could also be formed.[42] Useful information on the nature of the active sites has been also obtained by ^{13}C NMR microstructural characterization of the produced polypropylenes.[14,43−50] These analyses indicated that some active sites could interconvert in a time shorter than the average time of chain growth and that at least one of the active sites has an environment of C_1 symmetry.[47]

Although the whole framework is extremely complicated, some theoretical efforts have been attempted.[42,51−56] Most of the work concentrated on the chain growth reaction,[57−64] but these informative investigations did not consider in detail the origin of stereoselectivity, and limited efforts were dedicated to rationalize the role of different Lewis bases. The less investigated interaction between the Lewis bases and the $MgCl_2$ support substantially indicated that donors preferentially coordinate on the (110) lateral cut,[42,51−56] and it was speculated that

* Corresponding author. E-mail: acorrea@unisa.it.
† Università di Salerno.
‡ Basell Poliolefine Italia.

10.1021/ma071294c CCC: $37.00
Published on Web 11/16/2007

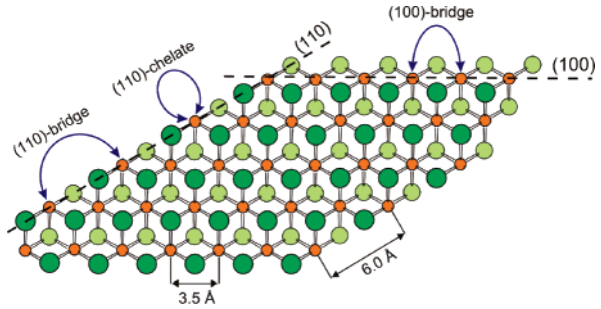

Figure 1. Schematic representation of a $MgCl_2$ monolayer. The Mg atoms are colored in orange. The Cl atoms above the Mg plane are dark green colored, whereas the Cl atoms below the Mg plane are light green colored. The (100) and (110) lateral cuts with 5- and 4-coordinated Mg atoms are indicated. The double arrow curves represent possible coordination modes of the donors of Chart 1.

Chart 1

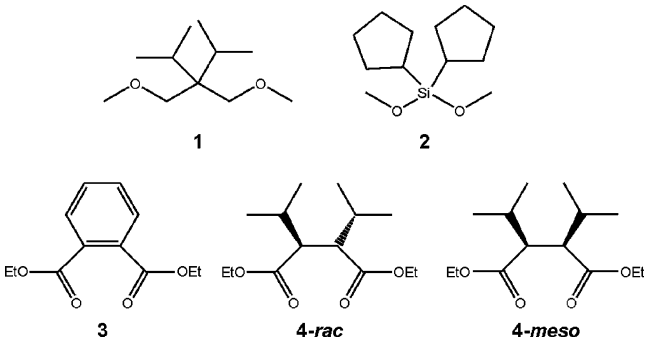

this preferential coordination could prevent formation of Ti species on the (110) lateral cut of $MgCl_2$, supposed to be poorly stereoselective.[56] Focusing on the performances of the most commonly used computational approaches, we recently found that almost all theoretical models substantially underestimate the experimental absolute complexation energy of prototype Lewis bases to $TiCl_4$, although relative complexation energies are calculated reasonably well.[36]

Considering that systematic studies on the interaction between different classes of donors and $MgCl_2$ are missing, and that detailed investigation of the possible role of the donors in determining stereoselectivity is missing as well, in this paper we present some of the results we obtained in recent years. The work is split in two parts. In the former we analyze possible interactions between the internal donors **1**, **2**, **3**, **4-*rac***, and **4-*meso*** of Chart 1 and the $MgCl_2$ support using a theoretical approach based on density functional theory, DFT. The donors are supposed to interact with the (100) and (110) lateral cuts of $MgCl_2$ as indicated in Figure 1. We considered only geometries in which both O atoms coordinate to Mg atoms, since coordination of the second O atom is clearly favored by entropic effects.

Two different adsorption modes are possible on the (110) lateral cut of a $MgCl_2$ monolayer: (i) chelated, if the two O atoms coordinate to the same Mg atom and (ii) bridged if the two O atoms coordinate to different Mg atoms. We label these adsorption modes, sketched in Figure 1, (110)-chelate and (110)-bridge, respectively. Differently, only the bridge coordination mode is possible on the (100) lateral cut, because only one coordinative vacancy is present in five-coordinated Mg atoms, see Figure 1.

We also considered donors coordination on Mg atoms located on different layers. This coordination mode, hereafter labeled as zipped coordination, is sketched in Figure 2. We considered the (110)-zip coordination mode because the distance between Mg atoms one on top of the other on stacked (110) layers is

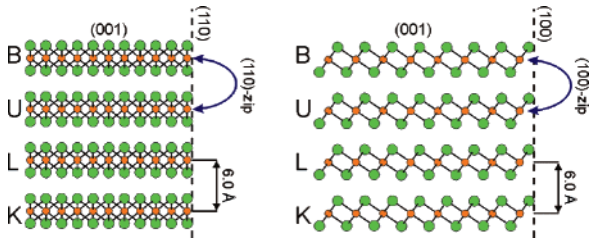

Figure 2. Schematic representation of stacked $MgCl_2$ monolayers. The Mg atoms are colored in orange, the Cl atoms in green. On the left, the (110) surface is represented and the double arrow curve represents the (110)-zip coordination mode. On the right, the (100) surface is represented and the double arrow curve represents the (100)-zip coordination mode.

Scheme 1

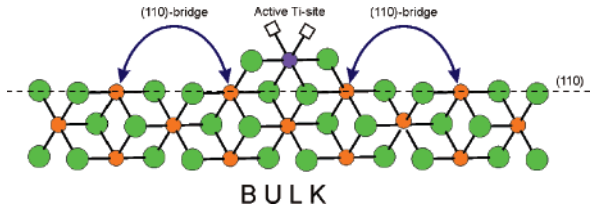

very similar to the distance between Mg atoms in the (110)-cut of a monolayer, about 6.0 Å. Of course, two Mg atoms on stacked (100) layers also are roughly 6.0 Å apart. However, because of the zigzag shape of the (100) surface, see Figure 2, we were unable to (100)-zip coordinate any donor. For this reason, the (100)-zip coordination mode is not further discussed. Donor coordination on (10*l*) lateral cuts of $MgCl_2$, as for example on the (102) cut,[20] was not considered because of the longer distance between Mg atoms located on different layers.

In the second part of this paper, we offer a very simple model to rationalize the influence of adsorbed donors on the stereo and regioselective behavior of possibly catalytically active Ti atoms. We focused on possible active Ti species adsorbed on the (110) lateral cut since the (110)-bridge coordination mode of the donors is particularly suited to strongly modify the steric properties of an isolated Ti atom adsorbed on this cut, see Scheme 1. Incidentally, (110)-bridge coordinated donors saturate the coordination sphere of the two Mg atoms on which the titanium−chloride species is adsorbed. The isolated Ti species of Scheme 1 was proposed years ago as a possibly active Ti atom which would produce a substantially atactic or slightly syndiotactic polypropylene.[65]

We conclude this section recalling that other active Ti species have been proposed.[57−63] In particular, Corradini and Guerra proposed that dimeric Ti species adsorbed on the (100) lateral cut would produce an isotactic polymer.[40,66−68] The main value of this Ti species is the ability to explain the fraction of isotactic polypropylene obtained in the absence of any donor and, even more important, for the introduction of the mechanism of the chiral orientation of the growing chain,[69] while the possible active species presented in this paper, instead, owe all their stereoselective behavior to the presence of the donors. Additionally, Busico proposed a three-site dynamic model that assumes adsorption/desorption of species near to the active Ti atoms. This results in a switch between active species with different stereo- and regioselective behaviors.[49]

Computational Details

Computational Details. The $MgCl_2$ support was described using the cluster method, an approach validated by Ziegler and co-workers.[61] All the DFT calculations were carried out using

the TURBOMOLE[70] package. Energies and geometries have been obtained at the BP86 level of theory.[71−73]

$MgCl_2$/Donor Interactions. Geometries of adsorbed donor molecules have been always fully optimized. To represent the (100) cut, a $(MgCl_2)_7$ cluster has been used. For the three different adsorption modes on the (110) cut, $(MgCl_2)_6$, $(MgCl_2)_9$, and $(MgCl_2)_{10}$ clusters have been used to represent the (110)-chelate, (110)-bridge, and (110)-zip, respectively. The $MgCl_2$ clusters have been kept fixed. The Mg−Cl distances and all the Cl−Mg−Cl angles have been set equal to X-ray values of 2.49 Å and 90°.[74] This corresponds to the simplifying assumption that the atoms on the surface present a structure close to that in the bulk of the crystal. While this assumption can result in an overestimation of the absolute coordination energies, calculations we performed in the past indicated that trends in relative coordination energies are preserved.[42,51−55] Since the scope of the present manuscript is to compare different donors, we believe that the rigid cluster approximation provides a reliable chemical scenario.The electronic configuration of the atoms was described by a triple-ζ basis set augmented with two polarization function (TURBOMOLE basis set TZVPP).[75] All coordination energies were corrected for basis set superposition error with the counterpoise approach of Boys and Bernardi.[76]

The donor adsorption energy, E_{Coord}, is calculated according to eq 1:

$$E_{Coord} = E_{Mg/D} - E^0_{Mg} - E^0_{D} \quad (1)$$

where $E_{Mg/D}$ is the energy of the system composed by a donor molecule bonded on the Mg_nCl_{2n} cluster, while E^0_{Mg} and E^0_{D} are the total energies of the Mg_nCl_{2n} cluster and of the free donor, respectively. For analysis purposes the donor adsorption energy E_{Coord} can be rewritten as in eq 2:

$$E_{Coord} = E_{Prep} + E_{Inter} \quad (2)$$

where $E_{Prep} = E_D - E^0_D$ only contains the energy required to deform a free donor molecule in a conformation suitable to be bonded on the surface (the $MgCl_2$ cluster being kept frozen). E_{Inter}, instead, is the interaction energy between the distorted donor and the Mg_nCl_{2n} cluster. In this framework E_{Prep} is positive by definition, whereas E_{Inter} is negative.

Active Sites Study. To model the (110) lateral cut, a $(MgCl_2)_{10}$ cluster has been used, to increase flexibility, and in the case of active species, we relaxed the four $MgCl_2$ units of the cluster surface which are involved in donors and titanium−chloride coordination. Because of the presence of a Ti(III) atom, unrestricted DFT calculations were performed in the case of the active species. The electronic configuration of Ti and Mg was described by a triple-ζ basis set augmented with one polarization function (TURBOMOLE basis set TZVP).[75] For H, C, and Cl atoms, a double-ζ quality basis set augmented with one polarization function was used (TURBOMOLE basis set SVP).[77]

Because of the size of the systems considered, full transition state searches could not be performed. Thus, transition states for primary and secondary propene insertion into the Ti−^{i}Bu bond were approximated through a linear scan of the potential energy surface in the region 2.10−2.25 Å of the new forming C−C bond with a step of 0.05 Å. All other degrees of freedom were optimized. This choice is based on the fact that the forming C−C bond in transition states for insertion of ethene or propene into Ti−alkyl bonds is almost invariably calculated to be in this range.[57,61−63,78] In each case the geometry higher in energy was considered to be a reasonable approximation to the real transition state. A similar approach was used by Ziegler and co-workers in the similarly difficult case of acrylates polymerization.[79]

Table 1. Absolute, E_{Coord}, and Relative, ΔE_{Coord}, Coordination Energies of CH_3COOCH_3 and CH_3OCH_3 to a Single $MgCl_2$ Fragment and to the (100) and (110) Lateral Cuts of $MgCl_2$

donor	$MgCl_2$ fragment	(110)-bridge	(100)-bridge
Absolute E_{Coord} (kcal/mol)			
CH_3COOCH_3 (sp^2 O)	−23.9	−26.5	−23.0
CH_3COOCH_3 (sp^3 O)	−13.9	−15.2	−8.6
CH_3OCH_3	−25.6	−25.5	−21.7
Relative ΔE_{Coord} (kcal/mol)			
CH_3COOCH_3 (sp^2 O)	0.0	0.0	0.0
CH_3COOCH_3 (sp^3 O)	10.0	11.3	14.4
CH_3OCH_3	−1.7	1.0	1.3

Results

Interaction $MgCl_2$/Donors. We start this section by considering coordination of the different type of O atoms present in the donors of Chart 1. Donors **1** and, somewhat similarly, **2** present etheric sp^3 O atoms, while **3** and **4** contain two chemically different O atoms, esteric sp^3 and carboxylic sp^2. Thus, we first considered coordination of the simplest ether and ester, namely, CH_3OCH_3 and CH_3COOCH_3, to a single $MgCl_2$ fragment and to both the (100) and (110) $MgCl_2$ lateral cuts.

Donors coordination to a single $MgCl_2$ fragment reflects the relative Lewis base strength of these O atoms (E_{Coord} of the O atoms: ether > carboxyl ≫ ester). Differently, the E_{Coord} for donors coordination to the (100) and (110) lateral cuts of the $MgCl_2$ clusters indicate that coordination of the carboxylic sp^2 O atom is favored by roughly 1 kcal/mol relative to coordination of the etheric sp^3 O atom and by roughly 10−15 kcal/mol relative to coordination of the esteric sp^3 O atom, see Table 1. Geometrical analysis indicates that short distances between the CH_3 groups of CH_3OCH_3 and Cl atoms of the $MgCl_2$ lateral cut are responsible for the reduced stability of the ether/$MgCl_2$ cluster interaction. Conversely, the alcoholic substituents of the ester can be easily folded away from the $MgCl_2$ surface. This feature is observed also in the case of coordination of the donors of Chart 1, compare structures (110)-chelate of **1** and **4-*meso***, reported in Figure 3. The conclusion is that esters coordinate more strongly than ethers to $MgCl_2$ surfaces, despite the higher basicity of ethers, and that coordination of esters occur exclusively through the carboxylic O atom. Finally, coordination on the (110) lateral cut is favored by roughly 3−5 kcal/mol relative to coordination on the (100) lateral cut, in agreement with the suggested more acidic behavior of the (110) lateral cut.[40]

Adsorption of Donors 1−4. The coordination energy of the donors of Chart 1 to the (100) and (110) lateral cuts of $MgCl_2$ are reported in Table 2. Independently of the coordination mode, adsorption of all the donors is remarkably favored. Even considering cluster relaxation effects, and a substantial unfavorable entropic contribution, the numbers of Table 2 indicate that all the Mg atoms at the $MgCl_2$ surface should be interacting with a Lewis base when the support is contacted with an excess of Lewis base.

In agreement with the results obtained for the simple models of Table 1, coordination of phthalates, **3**, and succinates, **4-*rac*** and **4-*meso***, is remarkably favored relative to coordination of 1,3-diethers, **1**, and of alkoxysilanes, **2**. Considering the E_{Coord} of CH_3OCH_3 and CH_3COOCH_3 (∼20−25 kcal/mol), E_{Coord} of donors **1**−**4** should be in the range of 40−50 kcal/mol. Differently, the E_{Coord} of donors **1**−**4** are always smaller than

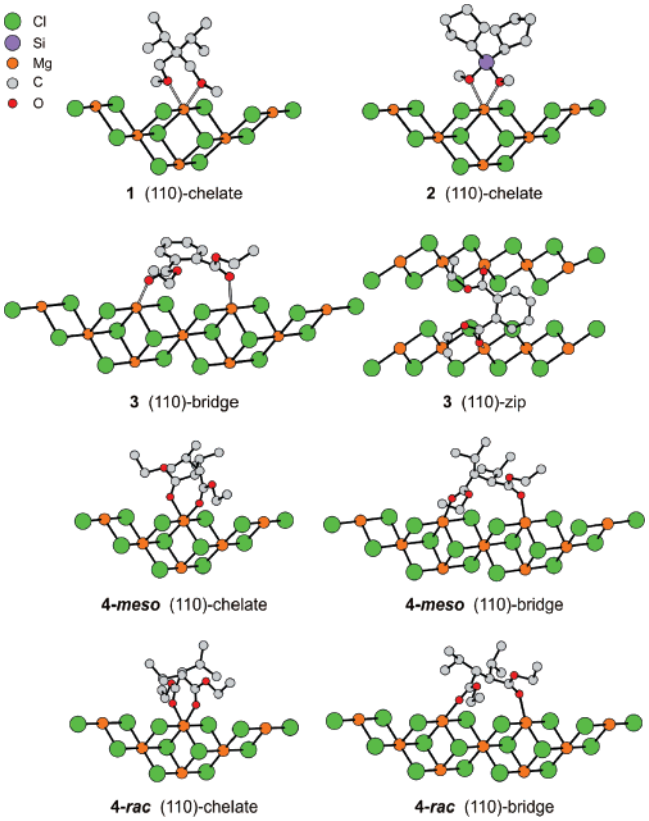

Figure 3. Representative geometries of coordinated Lewis bases to the (100) and (110) lateral cuts of $MgCl_2$.

Table 2. Absolute, E_{Coord}, and Relative, ΔE_{Coord}, Coordination Energies of the Lewis Bases of Chart 1 on the (100) and (110) Lateral Cuts of $MgCl_2$

donor	(110)-chelate	(110)-bridge	(110)-zip	(100)-bridge
	Absolute E_{Coord} (kcal/mol)			
1	−25.9	−13.4	−17.3	−14.8
2	−27.6	−18.3	−21.4	−16.5
3	−32.0	−34.2	−36.8	−32.2
4-*rac*	−32.1	−37.1	−28.7	−31.7
4-*meso*	−36.5	−35.1	−33.6	−32.6
	Relative ΔE_{Coord} (kcal/mol)			
1	0	12.6	8.6	11.1
2	0	9.2	6.1	11.1
3	0	−2.2	−4.9	−0.2
4-*rac*	0	−5.0	3.4	0.4
4-*meso*	0	1.4	2.9	3.8

40 kcal/mol, which indicates that the skeleton of the chelating donors reduces their coordination ability. Coordination of donors **1** and **2** is selective with a preference for the (110)-chelate coordination mode, with the (110) and (100)-bridge coordination modes roughly 10 kcal/mol higher in energy. Differently, for **3** and both **4-*rac*** and **4-*meso***, all the adsorption modes, including the (110)-zip that involves coordination on two vicinal $MgCl_2$ monolayers, are closer in energy. It is worthy to note that a stable (110)-zip coordination mode could induce the stacking of $MgCl_2$ monolayers along the (001) direction.

From a geometric point of view, the Mg−O distances are in the range of 2.2−2.4 Å independently of the donor or coordination mode, while the donor assumes a conformation with the alkyl substituents on the donor skeleton folded away from the $MgCl_2$ surface, see Figure 3. Only alkoxysilane **2** deviates from this behavior due to the very short Si< spacer that makes the bridge or zip coordination of **2** quite problematic. Indeed, these geometries substantially present only one O atom coordinated to the Mg atom.

Table 3. Relative Energies, in kcal/mol, of the Approximate Transition States, See Computational Detail Section, Corresponding to Primary (or 1,2) and Secondary (or 2,1) Insertion of Propene into the Ti−^{i}Bu Bond of the Models Depicted in Figure 4 (No Donor Column) and Figure 5 ((110)-Bridged Donor Column)

geometry	no donor	(110)-bridged donor
1,2-si	0.0	0.0
1,2-re	−0.2	3.1
2,1-re	1.3	1.4
2,1-si	1.1	4.5

Energy decomposition according to eq 2, reported in the Supporting Information, indicates that E_{Prep} of **1** and **3**, with a short spacer between the coordinating O atoms, increases in the order (110)-chelate < (100)-bridge < (110)-zip ≈ (110)-bridge. Donor **2** presents low E_{Prep} because of the limited flexibility of alkoxysilanes, while the rather low E_{Prep} of **3** is due to limited rotational flexibility around the aromatic C−C bond, which also prevents **3** to chelate effectively to a single Mg atom in the (110)-chelate geometry. Differently, because of the flexible four sp^3 C-atom spacer, both **4-*rac*** and **4-*meso*** show rather low E_{Prep}. This flexibility confers to succinates the unique ability to adopt a variety of conformations, and thus they can effectively coordinate to one single Mg atom as well as to Mg atoms that are 3.5 or 6.0 Å apart.

Nevertheless, the main conclusion of this section is that donors can be split into two classes. Only the (110)-chelate coordination mode is allowed to donors with a short spacer between the coordinating O atoms (diethers and alkoxysilanes) whereas donors with a longer spacer (phthalates and succinates) can adopt a variety of coordination modes.

Models of Possible Active Species. In the last part of the manuscript, we report on possible models of Ti active species and on the possible influence of Lewis bases on the stereo- and regioselectivity of these active species. We warn that these models are, of course, rather hypothetical as any model of active species in this peculiar field. However, we believe that the main concepts conveyed by these models could contribute to build a chemical scenario able to rationalize the experimental behavior.

We have considered mononuclear Ti species on the (110) lateral cut of $MgCl_2$. This active site was proposed by Corradini and co-workers. The active Ti(III) atom is 6-fold coordinated and sits hepitaxially on the $MgCl_2$ surface in a configuration similar to bulk Mg atoms (see Scheme 1). The resulting octahedrally coordinated Ti atom is chiral, and its chirality can be labeled Δ or Λ. For the sake of simplicity, in all the calculations we fixed the configuration of the Ti atom to be Δ.[69] All the energies discussed in this section are collected in Table 3.

The approximate transition states for primary and secondary propene insertion into the Ti−^{i}Bu bond of this model are sketched in Figure 4. The most favored transition state (Figure 4b) corresponds to primary insertion of *re*-propene on a (−) growing chain.[69] The transition state for primary insertion of the other propene enantioface (Figure 4a) corresponds to insertion of *si*-propene on a (+) growing chain. The energy difference between these two approximate transition states, $\Delta E^{\ddagger}_{Stereo}$, is a measure of the stereoselectivity of this active site. The very low $\Delta E^{\ddagger}_{Stereo}$ we calculated, 0.2 kcal/mol, is well below the accuracy that can be expected from this kind of calculation. Nevertheless, it clearly indicates that an isolated C_2-symmetric Ti atom on the (110) lateral cut of $MgCl_2$ is essentially nonstereoselective.

The approximate transition states for secondary propene insertion (Figure 4c,d) correspond to *re*- and *si*-propene insertion on a (+) growing chain, respectively. These two approximate

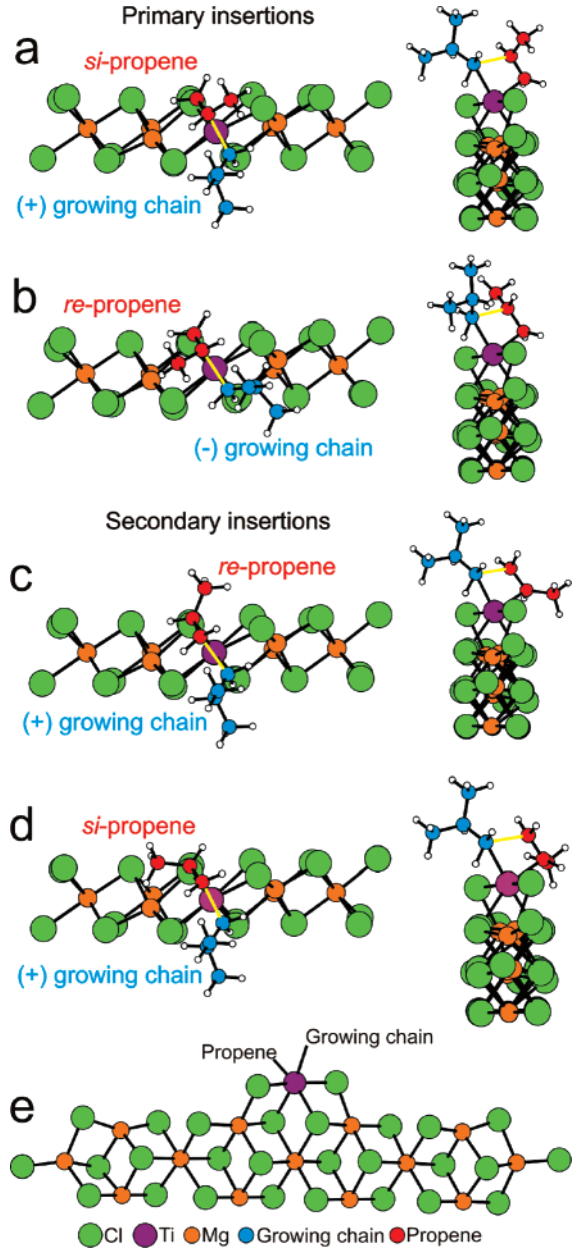

Figure 4. Top (left) and side (right) views of the transition states leading to primary, parts a and b, and secondary, parts c and d, propene insertion into the Ti−^{i}Bu bond. For the sake of clarity, in the top views only a part of the $MgCl_2$ cluster is reported. The cluster actually used is reported in part e.

transition states are about 1.1−1.3 kcal/mol higher in energy relative to the transition states leading to primary insertion. These energy differences, $\Delta E^{\ddagger}_{Regio}$, are a measure of the regioselectivity of this active site. The rather low $\Delta E^{\ddagger}_{Regio}$ we calculated for both propene enantiofaces indicates that an isolated C_2-symmetric Ti atom on the (110) lateral cut of $MgCl_2$ should introduce a large amount of regiomistakes into the polypropylene chain. Moreover, the small energy difference between the two transition states leading to secondary insertion, 0.2 kcal/mol, indicates that there is no preference for one of the two propene enantiofaces. In short, the polypropylene produced by an isolated and active Ti species on the (110) lateral cut of a monolayer should be substantially atactic, in agreement with previous molecular mechanics calculations by Corradini and co-workers,[57] and should present a rather high amount of nonenantioselective regiomistakes, in agreement with previous quantum mechanics calculations by Busico and Ziegler on similar models.[49,64]

An isolated Ti(III) active species on the (110) lateral cut of $MgCl_2$ can thus rationalize the large amount of substantially atactic polypropylene obtained with $MgCl_2$ supported catalytic systems in the absence of any Lewis base. Additionally, this active species can also rationalize the rather high amount of nonenantioselective regiomistakes recently described by Busico and co-workers through the NMR analysis of propene/ethene-[1-^{13}C] copolymers obtained with the catalytic system $MgCl_2/TiCl_4-AlR_3$ in the absence of any Lewis base.[49] As a final note, we specify that the $\Delta E^{\ddagger}_{Regio}$ we calculated, about 1.1−1.3 kcal/mol, underestimates the experimental value, about 2 kcal/mol. As already noticed, better agreement with the experimental results can be obtained if a hybrid DFT functional, as the B3LYP functional, is used.[80−82] B3LYP single point energy calculations on the structures of Figure 4a,c result in a $\Delta E^{\ddagger}_{Regio}$ of 1.7 kcal/mol. Although a better qualitative agreement with the experimental number is obtained with the B3LYP functional, the overall chemical scenario is substantially the same. For this reason, we decided to not use the B3LYP functional any further due to its computational cost on systems of this size.

To investigate the influence of adsorbed donors on the behavior of this active site, we coordinated two molecules of *rac*-1,4-dimethoxy-2,3-dimethyl succinate on both sides of the isolated Ti active species just discussed. On both sides, the coordination mode of the donor is (110)-bridge and it involves one Mg atom that also interacts with a Cl atom of the Ti species. The approximate transition states corresponding to primary and secondary propene insertion on this active site are reported in Figure 5.

The numbers reported in Table 3 clearly indicate that the donor strongly modifies the stereo- and regioselectivity of the active species. With a focus on primary insertion, the *si* enantioface of propene is clearly favored over the *re* enantioface and the $\Delta E^{\ddagger}_{Stereo}$ raises to 3.1 kcal/mol. The transition states for secondary insertion of the *re* and *si* enantiofaces of propene are 1.4 and 4.5 kcal/mol higher in energy relative to the favored primary insertion, respectively, which means that the $\Delta E^{\ddagger}_{Regio}$ is 1.4 kcal/mol. In short, the two donor molecules transform an otherwise nonselective site into a remarkably stereoselective site, while the effect on regioselectivity is rather strong for one propene enantioface but quite small for the other.

Examination of the structures of Figure 5 holds an explanation for these findings. The most stable transition state for primary insertion (Figure 5a) shows the most classical features which characterize the mechanism of the chiral orientation of the growing chain proposed by Corradini and co-workers for heterogeneous and homogeneous polymerization catalysts.[69] In order, they are (i) the growing chain assumes a chiral orientation, (+) in this case, to minimize steric interactions with the bulky succinates; (ii) the monomer inserts with the methyl group trans to (i.e., away from) the C_β and the following atoms of the growing chain, to minimize steric interactions with the growing chain.

Instead, the transition state leading to a stereomistake (Figure 5b) is disfavored by steric interactions between the (−) growing chain and one of the succinates. Given the overall C_2 symmetry of the Ti species in the presence of two succinate molecules, exactly the same geometrical arrangement of atoms would be present in the following step when, in the framework of the chain migratory mechanism, the relative coordination positions of the monomer and of the growing chain would be exchanged. Thus, this hypothesized active site would lead to an isotactic

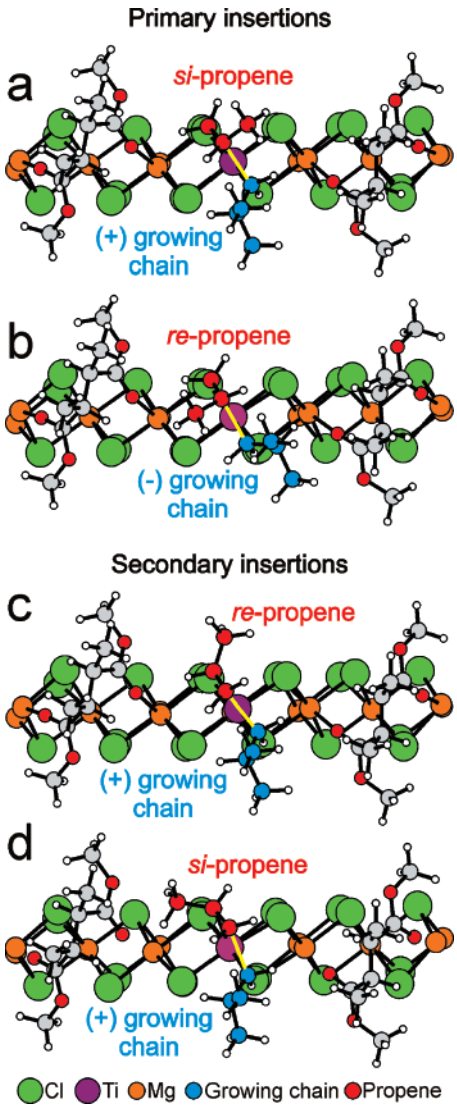

Figure 5. Top view of the transition states leading to primary, parts a and b, and secondary, parts c and d, propene insertion into the Ti−^{i}Bu bond. For the sake of clarity, in the top views only a part of the $MgCl_2$ cluster actually used is reported (see Figure 4). The Ti-active site is flanked by two *rac*-1,4-dimethoxy-2,3-dimethyl succinate molecules (110)-bridge coordinated.

polymer. This finding is in agreement with the well-known fact that a high amount of isotactic polypropylene is obtained only in the presence of a Lewis base, and with previous TREF analysis, which indicated that addition of donors significantly limits formation of aspecific sites and drastically promote formation of sites with highest isospecificity.[11,14,16,17,83]

The stereoselective behavior and the overall geometry of the active site in the presence of two Lewis base molecules around the Ti atom is very similar to the models developed to explain the isospecific behavior of bridged bisphenoxy−amine based homogeneous catalysts, which adds to similar analogies between homogeneous and heterogeneous catalysts proposed in the past.[69,84] All these species present an octahedrally coordinated metal atom in a C_2 symmetric coordination sphere. Stereoselectivity is provided by the X group in the structure of Scheme 2, which is a surface Cl atom in the models proposed for $TiCl_3$ and for $MgCl_2/TiCl_4$ in the absence of donors,[40,66−68] a bulky alkyl group in the bridged bisphenoxy−amine based homogeneous catalysts,[84−86] and a donor in the models presented in this paper.

Scheme 2

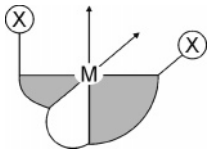

Scheme 3

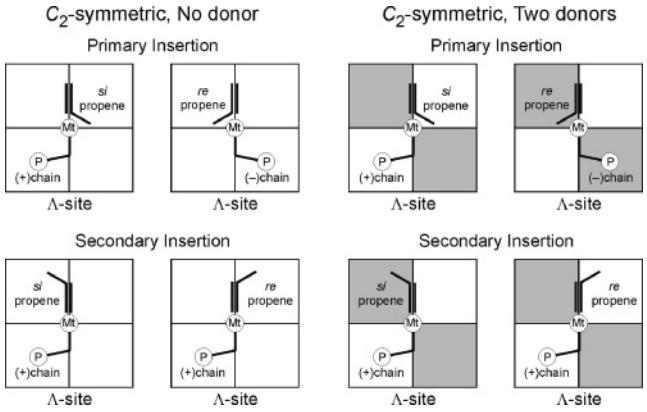

With a focus on regioselectivity, the adsorbed donors have a small effect on the insertion of the *re*-enantioface because the corresponding transition state (Figure 5c) presents a (+) orientation of the growing chain and the secondary inserting propene presents the methyl group far away from both donors. This explains the relatively small increase of $\Delta E^{\ddagger}_{\mathrm{Regio}}$ after inclusion of the two donor molecules.

Instead, the donor has a remarkable effect on the insertion of the *si*-enantioface because the corresponding transition state (Figure 5d) presents the methyl group of the secondary inserting propene very close to one of the donors. Thus, the donors destabilize only one of the two transition states leading to secondary propene insertion. The sharp conclusion is that the overall regioselectivity of the model is not changed substantially, but it is very enantioselective. Incidentally, the calculations indicate that opposite propene enantiofaces are favored in primary and secondary insertion. Our results are in agreement with previous quantum mechanics calculations of Busico and co-workers on a smaller system in which bulkiness around the Ti atom is provided by Cl atoms.[82]

Again, our model is in good agreement with the experimental characterization of propene/ethene-[1-^{13}C] copolymers obtained with the catalytic system $MgCl_2/TiCl_4-AlR_3$ in the presence of a dialkyl phthalate and of a 1,3-diether[50] and with the main conclusion of Busico and co-workers that the lower amount of regiomistakes in the presence of the donors is mostly related to higher enantioselectivity in the secondary insertions. Additionally, our finding that primary and secondary insertions occur with opposite enantiofaces also is in good agreement with the experimental results.

Discussion

As final comments we try to discuss the results using a more general quadrants representation we used in the past. The Ti active species without and with two coordinated donors are schematically sketched in the quadrants representation of Scheme 3. Gray quadrants represent regions sterically occupied by the donors. Of course, there are no gray quadrants if no donor is coordinated. In this case the growing chain is not forced to assume a chiral orientation, and thus primary insertion is nonstereoselective because the (−)chain/*re*-propene and (+)-

Scheme 4

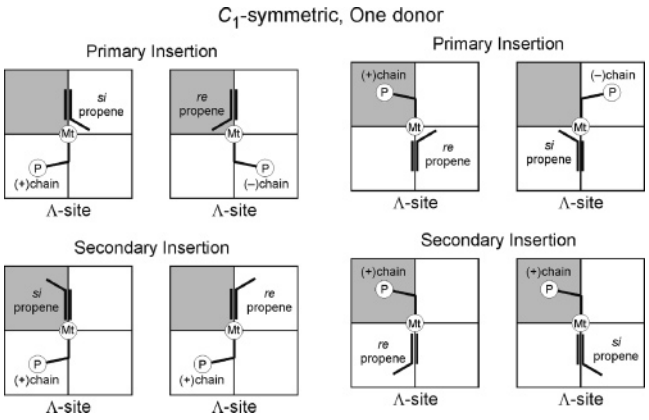

chain/*si*-propene combination of chiralities are almost of the same energy (top-left in Scheme 3). Secondary insertion is also nonstereoselective because both enantiofaces of a secondary inserting monomer can be accommodated on the active site without relevant steric interactions (bottom-left in Scheme 3).

Different is the case with two donors coordinated. In this case, the donors impose a chiral orientation to the growing chain and, in the case of an active site with a Λ configuration at the metal, the (−)chain/*re*-propene combination of chiralities is of higher energy relative to the (+)chain/*si*-propene combination (top-right in Scheme 3). Steric effects occur also in the insertion of a secondary propene molecule. In this case, the donors sterically destabilize insertion of a *si*-propene through direct interaction with the methyl group of the monomer. Thus also secondary insertion is stereoselective (bottom-right in Scheme 3).

The last possibility is that only one donor is coordinated close to the active Ti atom (see Scheme 4). In this case, the eventual stereoselectivity of the primary and secondary insertions depends on which side of the active Ti atom the donor is coordinated. If the donor is close to the monomer, primary insertion is nonstereoselective, while secondary insertion is remarkably stereoselective (Scheme 4, left). In the case where the donor is close to the growing chain, primary insertion is remarkably stereoselective, while secondary insertion is nonstereoselective (Scheme 4, right).

Thus, in the presence of only one coordinated donor, the structure of the resulting polypropylene will depend on the relative energy between the two situations depicted on the left and right sides of Scheme 4. If they present similar energy, within the framework of the chain migratory mechanism a hemiisotactic polymer[87] should be produced. A situation like this is observed in the polymerization of propene with C_1-symmetric metallocenes such as $Me_2C(3Me-Cp)(9-Flu)ZrCl_2$.[88,89] If the situations are of remarkably different energy, regular chain migration could be replaced by a regular back-skip of the growing chain (or chain-retention), so that insertion occurs always with the same disposition of the monomer and of the growing chain relative to the coordinated donor. If the situation with the growing chain close to the donor is more stable (Scheme 4, right side), an isotactic polypropylene will be produced. A situation like this has been proposed for possible Ti active species on lateral surfaces of α-$TiCl_3$, on the (100) lateral cut of $MgCl_2/TiCl_4$ supported catalysts, and is observed in the polymerization of propene with C_1-symmetric metallocenes such as $Me_2C(3-^tBu-Cp)(9-Flu)ZrCl_2$.[90,91]

Assuming reversible adsorption/desorption of the donors, the three static situations of Schemes 3 and 4 can be linked together

Scheme 5

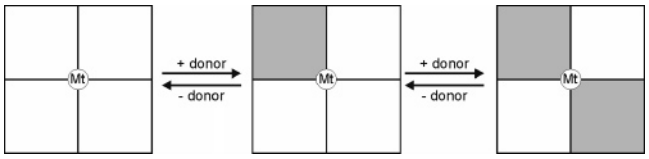

in the single dynamic model of Scheme 5 and the emerging picture corresponds to a specific application of the three-site dynamic model proposed by Busico on the basis of quantum mechanics calculations on a general model,[49,92] and supported by experiments on properly designed single-center bis(phenoxyamine)Zr catalysts.[84] In the framework of Busico's model, adsorption/desorption of species near to the active Ti atoms results in a switch between active species with different stereo- and regioselective behaviors, as sketched in Scheme 5. Moreover, it can be hypothesized that any conformational change in the adsorbed donor or partial dissociation of the donor (i.e., the donor remains coordinated with a single O atom) can also result in decreased stereoselectivity. This would enlarge the validity of the three-site mechanism.

As a final remark, we note that the variety of active species we proposed here (which are only the most easy guesses) are possible because the donor we considered, a succinate, can coordinate in many different geometries. Moreover, Ti active species could also be flanked by donors in different coordination modes, for example (110)-bridge on one side and (110)-zip on the other. We also remind that the (110)-chelate coordination mode was not considered, that we did not consider coordination of other species as the Al−alkyls, and that we did not consider possible active species on the (100) lateral cut. All these possibilities are of course unmanageable within a single manuscript.

Conclusions

In the first part of this manuscript we investigated the structure and energetic relative to coordination of several Lewis bases to $MgCl_2$ surfaces. The main conclusions we obtained are (i) All the Lewis bases we considered coordinate rather strongly to both the (100) and (110) lateral cuts. Although, only one coordination mode is possible on the (100) lateral cut, whereas several coordination modes are possible on the (110) lateral cut. Additionally, one of these coordination modes involves vicinal (110) monolayers. This coordination mode could favor the stacking of $MgCl_2$ monolayers. (ii) The short spacer between the coordinating O atoms of alkoxysilanes and 1,3-diethers substantially imposes the (110)-chelate coordination. Instead, in the case of phthalates and succinates, the four-atom spacer confers flexibility to the donors, which can assume a variety of coordination modes. This flexibility is particularly high for succinates and phthalates and could result in broader variety of active sites. This could rationalize the fact that larger M_w/M_n are observed with phthalate, as an internal donor, than with diether-containing catalysts.[11]

In the last part of this manuscript we investigated the stereo- and regioselective behavior of possible catalytically active models corresponding to titanium−chloride species adsorbed on the (110) lateral cut. We focused on this lateral cut because it is very easy to build models with a close proximity between the coordinated donors and the active Ti species. The main conclusions we obtained are (i) Isolated Ti species on the (110) monolayer would lead to a substantially atactic polyproplylene. The regioregularity of this polypropylene would not be particularly high, and the occasional regiomistakes would not be

enantioselective. The microstructure of this polymer is rather consistent with that of the "less-tactic" polypropylene obtained in the absence of any Lewis base. (ii) Ti species on the (110) monolayer flanked by two donors (110)-bridge coordinated would lead to a substantially isotactic polyproplylene. The regioregularity of this polypropylene would be reasonably high, and the occasional regiomistakes would be enantioselective. The microstructure of this polymer is rather consistent with that of the polypropylene obtained in the presence of a Lewis base as phthalate or 1,3-diether. A polypropylene with a similar microstructure would be produced also with the donors (110)-zip coordinated on vicinal $MgCl_2$ layers.

We believe that our models should not be taken as models for the "real active species" (in its broadest sense) but should be considered as examples of the variety of possible active species that can be formed by the interaction between the different components of the heterogeneous Ziegler−Natta catalysts. A comprehensive description of these catalytic systems should include all possible combinations of $MgCl_2$ lateral cuts and junctions between different lateral cuts, of differently adsorbed donors, of Al−alkyl and chloride species, and of isolated and clusterized titanium−chloride species. A task of this dimension needs to be puzzled out step by step.

Acknowledgment. We thank G. Guerra, University of Salerno, for useful discussions. This work was supported by CINECA (Progetti di Supercalcolo convenzione CINECA/INSTM). L.C. thanks Basell Polyolefins for continuous financial support.

Supporting Information Available: Details on the E_{Prep} and E_{Inter} contributions to E_{Coord} and Cartesian coordinates of all the structures. This material is available free of charge via the Internet at http://pubs.acs.org.

References and Notes

(1) Moore, E. P., Jr. *Polypropylene Handbook: Polymerization, Characterization, Properties, Applications*; Hanser Publishers: Munich, Germany, 1996.
(2) Albizzati, E.; Giannini, U.; Morini, G.; Galimberti, M.; Barino, L.; Scordamaglia, R. *Macromol. Symp.* **1995**, *89*, 73−89.
(3) Parodi, S.; Nocci, R.; Giannini, U.; Barbé, P. C.; Scata, U.; Montedison S.p.A. Components and Catalysts for the Polymerization of Olefins. Eur. Pat. EP0045977, February 17,1982.
(4) Barbè, C.; Cecchin, G.; Noristi, L. *Adv. Polym. Sci.* **1987**, *81*, 1−81.
(5) Morini, G.; Balbontin, G.; Basell Poliolefine Catalyst Components for the Polymerization of Olefins. Int. Pat. WO 2002030998, March 18, 2002.
(6) Seppälä, J. V.; Härkönen, M.; Luciani, L. *Makromol. Chem.* **1989**, *190*, 2535−2550.
(7) Chadwick, J. C.; Miedema, A.; Sudmeijer, O. *Macromol. Chem. Phys.* **1994**, *195*, 167−172.
(8) Chadwick, J. C.; van Kessel, G. M. M.; Sudmeijer, O. *Macromol. Chem. Phys.* **1995**, *196*, 1431−1437.
(9) Chadwick, J. C. In *Ziegler Catalysts*; Fink, G., Mülhaupt, R., Brintzinger, H.-H., Eds.; Springer: Berlin, Germany, 1995, pp 427−440.
(10) Chadwick, J. C.; Morini, G.; Balbontin, G.; Mingozzi, I.; Albizzati, E.; Sudmeijer, O. *Macromol. Chem. Phys.* **1997**, *198*, 1181−1188.
(11) Chadwick, J. C.; Morini, G.; Balbontin, G.; Camurati, I.; Heere, J. J. R.; Mingozzi, I.; Testoni, F. *Macromol. Chem. Phys.* **2001**, *202*, 1995−2002.
(12) Noristi, L.; Barbè, P. C.; Baruzzi, G. *Makromol. Chem.* **1991**, *192*, 1115−1127.
(13) Barbè, P. C.; Noristi, L.; Baruzzi, G. *Makromol. Chem.* **1992**, *193*, 229−241.
(14) Morini, G.; Albizzati, E.; Balbontin, G.; Mingozzi, I.; Sacchi, M. C.; Forlini, F.; Tritto, I. *Macromolecules* **1996**, *29*, 5770−5776.
(15) Xu, J.; Feng, L.; Yang, S.; Yang, Y.; Kong, X. *Macromolecules* **1997**, *30*, 7655−7660.
(16) Liu, B.; Nitta, T.; Nakatani, H.; Terano, M. *Macromol. Chem. Phys.* **2003**, *204*, 395−402.
(17) Matsuoka, H.; Liu, B.; Nakatani, H.; Terano, M. *Macromol. Rapid Commun.* **2001**, *22*, 326−328.
(18) Rodriguez, L. A. M.; van Looy, H. M. *J. Polym. Sci., Part A: Polym. Chem.* **1966**, *4*, 1951−1968.
(19) Galli, P.; Luciani, L.; Cecchin, G. *Angew. Makromol. Chem.* **1981**, *94*, 63−89.
(20) Giannini, U.; Giunchi, G.; Albizzati, E. *NATO ASI Ser., Ser. C* **1987**, *215*, 473−484.
(21) Chien, J. C. W.; Kuo, C.-I. *J. Polym. Sci., Part A: Polym. Chem.* **1986**, *24*, 1779−1818.
(22) Chien, J. C. W.; Bres, P. *J. Polym. Sci., Part A: Polym. Chem.* **1986**, *24*, 1967−1988.
(23) Chien, J. C. W.; Weber, S.; Hu, Y. In *Transition Metals and Organometallics as Catalysts for Olefin Polymerization*; Kaminsky, W., Sinn, H., Eds.; Springer-Verlag: Berlin, Heidelberg, Germany, 1988, p 45.
(24) Brant, P.; Tornqvist, E. G. M. *Inorg. Chem.* **1986**, *25*, 3776−3779.
(25) Brant, P.; Speca, A. N.; Johnston, D. C. *J. Catal.* **1988**, *113*, 250−255.
(26) Mori, H.; Tashino, K.; Terano, M. *Macromol. Rapid Commun.* **1995**, *16*, 651−657.
(27) Mori, H.; Sawada, M.; Higuchi, T.; Hasebe, K.; Otsuka, N.; Terano, M. *Macromol. Rapid Commun.* **1999**, *20*, 245−250.
(28) Mori, H.; Hasebe, K.; Terano, M. *J. Mol. Catal. A: Chem.* **1999**, *140*, 165−172.
(29) Mori, H.; Saito, H.; Yamahiro, M.; Kono, H.; Terano, M. *Macromol. Chem. Phys.* **1998**, *199*, 613−618.
(30) Mori, H.; Iguchi, H.; Hasebe, K.; Terano, M. *Macromol. Chem. Phys.* **1997**, *198*, 1249−1255.
(31) Bukatov, G. D.; Goncharov, V. S.; Zakharov, V. A. *Macromol. Chem. Phys.* **1995**, *196*, 1751−1759.
(32) Bukatov, G. D.; Zakharov, V. A. *Macromol. Chem. Phys.* **2001**, *202*, 2003−2009.
(33) Potapov, A. G.; Kriventsov, V. V.; Kochubey, D. I.; Bukatov, G. D.; Zakharov, V. A. *Macromol. Chem. Phys.* **1997**, *198*, 3477−3484.
(34) Sergeev, S. A.; Poluboyarov, V. A.; Zakharov, V. A.; Anufrienko, V. F.; Bukatov, G. D. *Makromol. Chem.* **1985**, *186*, 243.
(35) Potapov, A. G.; Zakharov, V. A.; Mikenas, T. B.; Sergeev, S. A.; Volodin, A. M. *Macromol. Chem. Phys.* **1997**, *198*, 2867−2873.
(36) Cavallo, L.; Del Piero, S.; Ducéré, J.-M.; Fedele, R.; Melchior, A.; Morini, G.; Piemontesi, F.; Tolazzi, M. *J. Phys. Chem. C* **2007**, *111*, 4412−4419.
(37) Brambilla, L.; Zerbi, G.; Piemontesi, F.; Nascetti, S.; Morini, G. *J. Mol. Catal. A: Chem.* **2007**, *263*, 103−111.
(38) Trubitsyn, D. A.; Zakharov, V. A.; Zakharov, I. I. *J. Mol. Catal. A: Chem.* **2007**, *270*, 164−170.
(39) Auriemma, F.; Talarico, G.; Corradini, P. In *Progress and Development of Catalytic Olefin Polymerization*; Sano, T., Uozumi, T., Nakatani, H., Terano, M., Eds.; Technology and Education Publishers: Tokyo, Japan, 2000, p 7−15.
(40) Corradini, P.; Barone, V.; Fusco, R.; Guerra, G. *Gazz. Chim. Ital.* **1983**, *113*, 601−607.
(41) Giannini, U.; Giunchi, G.; Albizzati, E.; Barbè, P. C. In *Recent Advances in Mechanistic and Synthetic Aspects of Polymerization*; Fontanille, M., Guyot, A., Eds.; Reidel D. Publishing Co.: Boston, MA, 1987, p 473.
(42) Monaco, G.; Toto, M.; Guerra, G.; Corradini, P.; Cavallo, L. *Macromolecules* **2000**, *33*, 8953−8962.
(43) Zambelli, A.; Locatelli, P.; Bajo, G.; Bovey, F. A. *Macromolecules* **1975**, *8*, 687−689.
(44) Busico, V.; Corradini, P.; De Martino, L. *Makromol. Chem., Rapid Commun.* **1990**, *11*, 49−54.
(45) Paukkeri, R.; Lehtinen, A.; Väänänen, T. *Polymer* **1993**, *34*, 2488−2494.
(46) Busico, V.; Cipullo, R.; Corradini, P.; Landriani, L.; Vacatello, M.; Segre, A. L. *Macromolecules* **1995**, *28*, 1887−1892.
(47) Randall, J. C. *Macromolecules* **1997**, *30*, 803−816.
(48) Busico, V.; Cipullo, R.; Talarico, G.; Segre, A. L.; Chadwick, J. C. *Macromolecules* **1997**, *30*, 4786−4790.
(49) Busico, V.; Cipullo, R.; Polzone, C.; Talarico, G.; Chadwick, J. C. *Macromolecules* **2003**, *36*, 2616−2622.
(50) Busico, V.; Chadwick, J. C.; Cipullo, R.; Ronca, S.; Talarico, G. *Macromolecules* **2004**, *37*, 7437−7443.
(51) Puhakka, E.; Pakkanen, T. T.; Pakkanen, T. A. *Surf. Sci.* **1995**, *334*, 289−294.
(52) Puhakka, E.; Pakkanen, T. T.; Pakkanen, T. A. *J. Mol. Catal. A: Chem.* **1997**, *120*, 143−147.
(53) Puhakka, E.; Pakkanen, T. T.; Pakkanen, T. A. *J. Phys. Chem. A* **1997**, *101*, 6063−6068.
(54) Puhakka, E.; Pakkanen, T. T.; Pakkanen, T. A. *J. Mol. Catal. A: Chem.* **1997**, *123*, 171−178.
(55) Puhakka, E.; Pakkanen, T. T.; Pakkanen, T. A.; Iiskola, E. *J. Organomet. Chem.* **1996**, *511*, 19−27.

(56) Toto, M.; Morini, G.; Guerra, G.; Corradini, P.; Cavallo, L. *Macromolecules* **2000**, *33*, 1134−1140.
(57) Cavallo, L.; Guerra, G.; Corradini, P. *J. Am. Chem. Soc.* **1998**, *120*, 2428−2436.
(58) Boero, M.; Parrinello, M.; Terakura, K. *J. Am. Chem. Soc.* **1998**, *120*, 2746−2752.
(59) Boero, M.; Parrinello, M.; Hüffer, S.; Weiss, H. *J. Am. Chem. Soc.* **2000**, *122*, 501−509.
(60) Boero, M.; Parrinello, M.; Weiss, H.; Hüffer, S. *J. Phys. Chem. A* **2001**, *105*, 5096−5105.
(61) Seth, M.; Margl, P. M.; Ziegler, T. *Macromolecules* **2002**, *35*, 7815−7829.
(62) Seth, M.; Ziegler, T. *Macromolecules* **2003**, *36*, 6613−6623.
(63) Seth, M.; Ziegler, T. *Macromolecules* **2004**, *37*, 9191−9200.
(64) Flisak, Z.; Ziegler, T. *Macromolecules* **2005**, *38*, 9865−9872.
(65) Corradini, P.; Guerra, G.; Barone, V. *Eur. Polym. J.* **1984**, *20*, 1177.
(66) Corradini, P.; Barone, V.; Fusco, R.; Guerra, G. *Eur. Polym. J.* **1979**, *15*, 1133−1141.
(67) Corradini, P.; Guerra, G.; Fusco, R.; Barone, V. *Eur. Polym. J.* **1980**, *16*, 835−842.
(68) Corradini, P.; Barone, V.; Fusco, R.; Guerra, G. *J. Catal.* **1982**, *77*, 32−42.
(69) Corradini, P.; Guerra, G.; Cavallo, L. *Acc. Chem. Res.* **2004**, *37*, 231−241.
(70) Ahlrichs, R.; Bär, M.; Häser, M.; Horn, H.; Kölmel, C. *Chem. Phys. Lett.* **1989**, *162*, 165−169.
(71) Becke, A. D. *Phys. Rev. A* **1988**, *38*, 3098−3100.
(72) Perdew, J. P. *Phys. Rev. B* **1986**, *33*, 8822−8824.
(73) Perdew, J. P. *Phys. Rev. B* **1986**, *34*, 7406−7406.
(74) Partin, D. E.; O'Keeffe, M. *J. Solid State Chem.* **1991**, *95*, 176−183.
(75) Schäfer, A.; Huber, C.; Ahlrichs, R. *J. Chem. Phys.* **1994**, *100*, 5829−5835.
(76) Boys, S. F.; Bernardi, F. *Mol. Phys.* **1970**, *19*, 553−559.
(77) Schäfer, A.; Horn, H.; Ahlrichs, R. *J. Chem. Phys.* **1992**, *97*, 2571−2574.
(78) Woo, T. K.; Margl, P. M.; Blöchl, P. E.; Ziegler, T. *J. Am. Chem. Soc.* **1996**, *118*, 13021−13030.
(79) Tomasi, S.; Weiss, H.; Ziegler, T. *Organometallics* **2006**, *25*, 3619−3630.
(80) Becke, A. D. *J. Chem. Phys.* **1993**, *98*, 5648−5652.
(81) Becke, A. D. *J. Chem. Phys.* **1996**, *104*, 1040−1046.
(82) Lee, C.; Yang, W.; Parr, R. G. *Phys. Rev. B* **1988**, *37*, 785−789.
(83) Kono, H.; Mori, H.; Terano, M.; Nakatani, H.; Nishiyama, I. *J. Appl. Polym. Sci.* **2002**, *83*, 2976−2983.
(84) Busico, V.; Cipullo, R.; Ronca, S.; Budzelaar, P. H. M. *Macromol. Rapid Commun.* **2001**, *22*, 1405−1410.
(85) Tshuva, E. Y.; Goldberg, I.; Kol, M. *J. Am. Chem. Soc.* **2000**, *122*, 10706−10707.
(86) Busico, V.; Cipullo, R.; Friederichs, N.; Ronca, S.; Talarico, G.; Togrou, M.; Wang, B. *Macromolecules* **2004**, *37*, 8201−8203.
(87) Farina, M.; Di Silvestro, G.; Sozzani, P. *Macromolecules* **1993**, *26*, 946−950.
(88) Ewen, J. A.; Elder, M. J.; Jones, R. L.; Haspeslagh, L.; Atwood, J. L.; Bott, S. G.; Robinson, K. *Makromol. Chem., Macromol. Symp.* **1991**, *48/49*, 253−295.
(89) Herfert, N.; Fink, G. *Makromol. Chem., Macromol. Symp.* **1993**, *66*, 157−178.
(90) Kleinschmidt, R.; Reffke, M.; Fink, G. *Macromol. Rapid Commun.* **1999**, *20*, 284−288.
(91) Ewen, J. A.; Elder, M. J. In *Ziegler Catalysts*; Fink, G., Mülhaupt, R., Brintzinger, H.-H., Eds.; Springer-Verlag: Berlin, Germany, 1995, p 99.
(92) Busico, V.; Cipullo, R.; Monaco, G.; Talarico, G.; Vacatello, M.; Chadwick, J. C.; Segre, A. L.; Sudmeijer, O. *Macromolecules* **1999**, *32*, 4173−4182.

MA071294C